

Enhanced Optical and Electrical Properties of TiO₂ Buffered IGZO/TiO₂ Bi-Layered Films

Hyun-Joo Moon and Daeil Kim*

School of Materials Science and Engineering, University of Ulsan, Ulsan 44610, Republic of Korea

Abstract: In and Ga doped ZnO (IGZO, 100-nm thick) thin films were deposited by radio frequency magnetron sputtering without intentional substrate heating on a bare glass substrate and a TiO₂-deposited glass substrate to determine the effect of the thickness of a thin TiO₂ buffer layer on the structural, optical, and electrical properties of the films. The thicknesses of the TiO₂ buffer layers were 5, 10 and 15 nm, respectively. As-deposited IGZO films with a 10 nm-thick TiO₂ buffer layer had an average optical transmittance of 85.0% with lower resistivity ($1.83 \times 10^{-2} \Omega \text{ cm}$) than that of IGZO single layer films. The figure of merit (FOM) reached a maximum of $1.44 \times 10^{-4} \Omega^{-1}$ for IGZO/10 nm-thick TiO₂ bi-layered films, which is higher than the FOM of $6.85 \times 10^{-5} \Omega^{-1}$ for IGZO single layer films. Because a higher FOM value indicates better quality transparent conducting oxide (TCO) films, the IGZO/10 nm-thick TiO₂ bi-layered films are likely to perform better in TCO applications than IGZO single layer films.

(Received January 19, 2016; Accepted March 20, 2016)

Keywords: thin films, sputtering, optical properties, electrical properties, AFM.

1. INTRODUCTION

There is considerable interest in using metal-doped ZnO films such as AZO [1], GZO [2], and IGZO [3] films as transparent conducting oxide (TCO) layers for transparent electrodes because of their high optical transmittance in the visible wavelength range and greater chemical stability compared to conventional Sn-doped In₂O₃ (ITO) films.

Among these films, IGZO films have been used as an active layer in transparent thin film transistors (TTFTs) because the films can be deposited onto large area substrates as a uniform amorphous phase while retaining high carrier mobility [4]. However, it has also been reported that a relatively high substrate temperature or post-deposition annealing is required to obtain IGZO films with simultaneous optimal transparency and low resistivity [5].

One way to improve the optical and electrical properties of IGZO films without substrate heating is to use IGZO/metal/IGZO (OMO) structures [6], which have lower resistivity than IGZO single layer films. Another strategy that has been used to improve the electrical properties of IGZO films has been to insert an oxide buffer layer under the IGZO film [3].

In this study, IGZO thin films were deposited by radio frequency (RF) magnetron sputtering on glass substrate with and without a TiO₂ buffer layer, and then the effects of the TiO₂ buffer layer thickness on the optical and electrical properties of the IGZO films were investigated using X-ray diffraction (XRD), atomic force microscopy (AFM), Hall effect measurements, UV-visible spectrophotometry, and UV photoelectron spectroscopy (UPS).

2. EXPERIMENTAL PROCEDURES

IGZO single layer and IGZO/TiO₂ bi-layered films were deposited by RF magnetron sputtering on glass substrate (Corning 1797, $2 \times 2 \text{ cm}^2$) without intentional substrate heating. Both IGZO (In₂O₃ : Ga₂O₃ : ZnO = 1:1:1 at%) and TiO₂ targets had 3-inch diameters. Glass substrates were degreased in a dilute detergent solution, rinsed in de-ionized water, and blown dry in nitrogen gas before they were set on the substrate holder in the chamber. The distance between the target and substrate was kept at 60 mm. Prior to deposition, the sputter chamber was evacuated to 6.0×10^{-7} Torr and then 10 sccm Argon (Ar) gas was injected to achieve an optimized working pressure of 1.0×10^{-3} Torr. Table 1 shows the experimental conditions for IGZO film and TiO₂ buffer layer

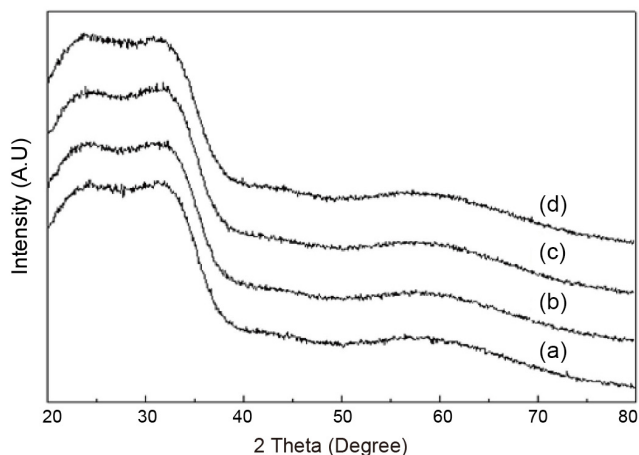
*Corresponding Author: Daeil Kim

[Tel: 82-52-259-22443, E-mail: dskim84@ulsan.ac.kr]

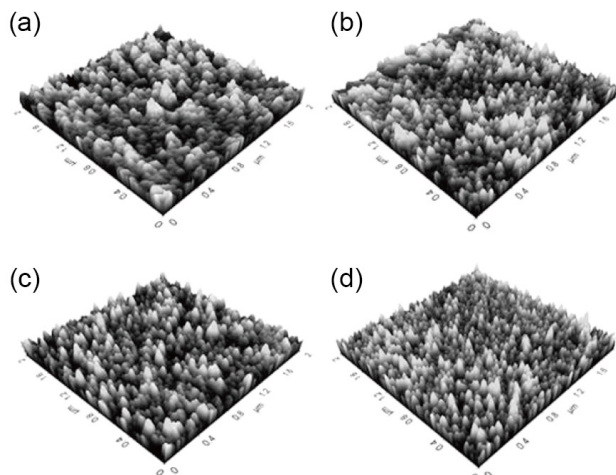
Copyright © The Korean Institute of Metals and Materials

Table 1. The experimental conditions for IGZO film and TiO₂ buffer layer deposition.

Parameters	Condition
Base pressure (Torr)	6.0×10^{-7}
Deposition pressure (Torr)	1.0×10^{-3}
IGZO target RF Power (W/cm ²)	2.5
TiO ₂ target RF Power (W/cm ²)	2.5
Ar gas flow rate (sccm)	10
Film thickness (nm)	IGZO: 100 TiO ₂ : 5, 10, 15
Deposition rate (nm/min)	IGZO: 3.4, TiO ₂ : 1.1

**Fig. 1.** The XRD patterns of the IGZO single layer and IGZO/TiO₂ bi-layered films: (a) 100 nm-thick IGZO films, (b) IGZO/5 nm-thick TiO₂ films, (c) IGZO/10 nm-thick TiO₂ films, and (d) IGZO/15 nm-thick TiO₂ films.

deposition. The deposition rates of the IGZO and TiO₂ films were evaluated with a surface profiler (Dektak-150, Varian) and the crystallinity of the films was investigated by XRD (X'pert PRO MRD, Phillips) analysis at the Korea Basic Science Institute (KBSI, Daegu Center). Optical transmittance in the visible wavelength region (400-700 nm) was determined using a UV-Vis. spectrophotometer (Cary 100 Cone, Varian). Variations in surface morphology ($2 \times 2 \mu\text{m}^2$ scanning area) and root mean square (RMS) roughness of the films were characterized by AFM [7] with the microscope operated in contact mode (XE-100, Park Systems). Electrical properties of the films were investigated by Hall effect measurements employing the Van der Pauw technique (HMS-3000, Ecopia). The opto-electrical performances of IGZO and IGZO/TiO₂ films as TCO electrodes were compared using the figure of merit (FOM). In addition, the

**Fig. 2.** Surface morphology and RMS roughness of the IGZO single layer and IGZO/TiO₂ bi-layer films: (a) 100 nm-thick IGZO films, (b) IGZO/5 nm-thick TiO₂ films, (c) IGZO/10 nm-thick TiO₂ films, and (d) IGZO/15 nm-thick TiO₂ films.

influence of the TiO₂ buffer layer on the work function of IGZO films was evaluated by UPS analysis.

3. RESULTS AND DISCUSSION

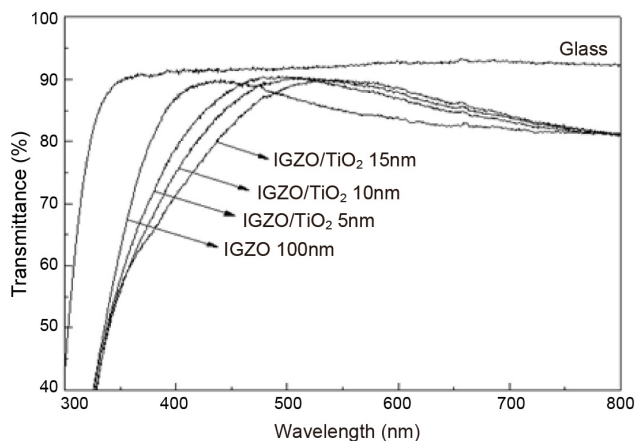
Figure 1 shows the XRD patterns of the IGZO single layer and IGZO/TiO₂ bi-layered films. The observed broad peak in the range of 20° to 40° is an amorphous halo-peak contributed by the IGZO film [3]. This means that IGZO films with the composition of In:Ga:Zn = 1:1:1 at% have an amorphous crystal structure.

Kim et al. reported that when the annealing temperature was below 600 °C, no crystalline peaks were present in the XRD pattern of IGZO films [8]. Based on these previous reports and the XRD patterns shown in Fig. 1, it appears that crystal growth did not occur for the IGZO/TiO₂ films deposited at room temperature.

Surface morphologies and RMS roughness of the IGZO single layer and IGZO/TiO₂ films with different TiO₂ buffer layer thicknesses are shown in Fig. 2. Surface roughness of the TCO films is an important determinant of their optical and electrical properties. The RMS roughness of the IGZO single layer film (1.5 nm) was higher than that of the IGZO/TiO₂ films. The presence of a TiO₂ buffer layer appeared to

Table 2. The electrical properties of the IGZO single layer and IGZO/TiO₂ bi-layered films.

Films	Carrier density ($\times 10^{19} \text{ cm}^{-3}$)	Mobility ($\text{cm}^2 \text{ V}^{-1} \text{ s}^{-1}$)	Resistivity ($\times 10^{-2} \Omega \text{ cm}$)
IGZO 100 nm	4.98	4.11	3.05
IGZO/TiO ₂ 5 nm	5.35	4.53	2.58
IGZO/TiO ₂ 10 nm	6.14	5.54	1.83
IGZO/TiO ₂ 15 nm	2.24	8.77	3.18

**Fig. 3.** The optical transmittance for IGZO single layer and IGZO/TiO₂ bi-layered films.

enhance the flatness of the IGZO/TiO₂ films. This indicates that the TiO₂ buffer layer grew preferably in sunken and defective regions of the substrate during deposition.

Thus, the IGZO/TiO₂ films had a flatter surface than the IGZO single layer films. The IGZO films with a 15 nm-thick TiO₂ buffer layer had a lower RMS roughness value (0.8 nm) than the other films prepared in this study. In a previous study, we reported similar results; a TiO₂ buffer layer resulted in the decreased RMS roughness of the upper GZO film in the context of GZO/TiO₂ bi-layered films [9].

Table 2 shows the influence of the TiO₂ buffer layer on the electrical properties of the films. IGZO/10 nm-thick TiO₂ films had a lower resistivity ($1.83 \times 10^{-2} \Omega \text{ cm}$) than IGZO single layer films due to increases in both carrier concentration and mobility in the former. The highest mobility of $8.77 \text{ cm}^2 \text{ V}^{-1} \text{ s}^{-1}$ was observed for IGZO/15 nm-thick TiO₂ film; we attributed this to the flat surface morphology of the films, as shown in Fig. 2.

Figure 3 shows the optical transmittance of the IGZO and

Table 3. The comparison of optical and electrical properties of IGZO single layer and IGZO/TiO₂ bi-layered films.

Films	Sheet resistance [Ω/\square]	Transmittance [%]	Figure of merit [$\times 10^{-5} \Omega^{-1}$]
IGZO 100 nm	3050	85.5	6.85
IGZO/TiO ₂ 5 nm	2457	86.9	9.99
IGZO/TiO ₂ 10 nm	1664	86.6	14.4
IGZO/TiO ₂ 15 nm	2765	85.8	7.82

IGZO/TiO₂ films. The average transmittance in the visible range was about 85.5% for the IGZO film, while the transmittance of IGZO/10 nm-thick TiO₂ film was about 86.6%.

Optical and electrical properties of the films are compared in Table 3. The figure of merit (FOM) is an important index for evaluating the performance of transparent conducting oxide (TCO) films [10]. FOM is defined as

$$\text{FOM} = T^{10} / R_s$$

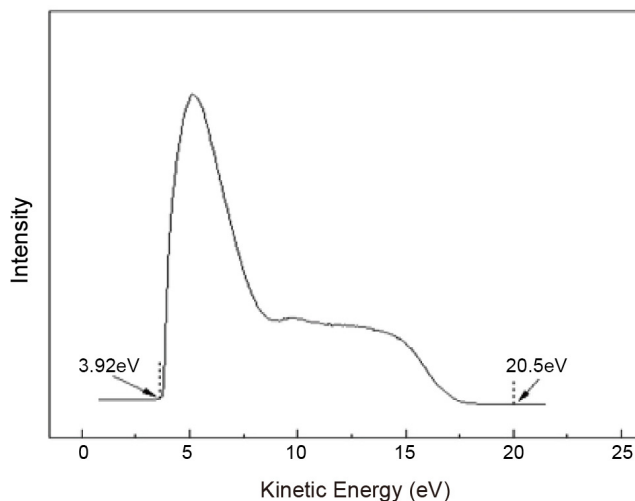
where T is the optical transmittance and R_s is the sheet resistance. The FOM reached a maximum of $1.44 \times 10^{-4} \Omega^{-1}$ for IGZO films with a 10 nm-thick TiO₂ buffer layer, which is higher than the FOM of $6.85 \times 10^{-5} \Omega^{-1}$ for IGZO single layer films. Because a higher FOM value indicates a better quality TCO film, the IGZO film with a 10 nm-thick TiO₂ buffer layer will likely perform better in TCO applications than IGZO single layer films.

The high work function of TCO films, which is close to the value of the highest occupied molecular orbital (HOMO) of the organic layer, allows hole injection from TCO to the organic layer of an organic light-emitting diode (OLED), which results in a decrease in the turn-on voltage of the OLED [9]. However, the work function of conventional ITO films is lower than the HOMO of the organic layer of OLEDs. Thus, several techniques have been developed to increase the work function of ITO [11].

Figure 4 shows the kinetic energy cut-off spectra obtained for the IGZO/10 nm-thick TiO₂ film. This allowed determination of the work function values directly from the spectra by fitting straight lines into their kinetic energy cut-offs and determining the intersections with the baselines of the

Table 4. Comparison of work function of the ITO/Ni/ITO trilayer, IGZO single layer and IGZO/TiO₂ bi-layered films.

Films	Work function (eV)
ITO/Ni/ITO	4.51 [11]
IGZO	4.10 [This study]
IGZO/TiO ₂ 10 nm	4.61 [This study]

**Fig. 4.** The kinetic energy cut-off spectra obtained from the IGZO/10 nm-thick TiO₂ bi-layered films.

spectra. The work functions of ITO/Ni/ITO trilayer [11], IGZO single layer, and IGZO/TiO₂ bi-layered films are compared in Table 4. The IGZO/10 nm-thick TiO₂ films had a higher work function (4.61 eV) than the other films. Thus, the addition of a TiO₂ buffer layer is a useful strategy to increase the work function of IGZO films.

4. CONCLUSIONS

Both IGZO single layer and IGZO/TiO₂ bi-layered films were deposited by RF magnetron sputtering on glass substrates without intentional substrate heating.

From AFM observations, it was apparent that the TiO₂ buffer layer enhanced the flatness of the IGZO/TiO₂ films, and the figure of merit of the IGZO/TiO₂ films reached a

maximum value of $1.18 \times 10^{-4} \Omega^{-1}$, which was higher than that of the IGZO films. In addition, IGZO/10 nm-thick TiO₂ films had a higher work function than IGZO single layer films.

The observed results indicated that the structural, optical, and electrical properties of the IGZO films were dependent on the TiO₂ buffer layer. The 10 nm-thick TiO₂ buffer layer in IGZO/TiO₂ films yielded films with better opto-electrical performance than IGZO single layer films.

ACKNOWLEDGEMENT

This work was supported by the Human Resource Training Program for Regional Innovation and Creativity through the Ministry of Education and National Research Foundation of Korea (No. NRF-2013H1B8A2032122).

REFERENCES

1. S. J. Kim, K. Choi, S. Y. Choi and *Korean J. Met. Mater.* **53**, 890 (2015).
2. Y. S. Kim, S. B. Heo, H. M. Lee, Y. J. Lee, I. S. Kim, M. S. Kang, D. H. Choi, B. H. Lee, M. G. Kim and D. Kim, *Appl. Surf. Sci.* **258**, 3903 (2012).
3. S. H. Kim and D. Kim, *Ceram. Int.* **41**, 2770 (2015).
4. M. F. A. M. van Hest, M. S. Dabney, J. D. Perkins, D. S. Ginley and M. P. Taylor, *Appl. Phys. Lett.* **87**, 032111 (2005).
5. J. H. Jeon, T. K. Gong, Y. M. Kong, H. M. Lee and D. Kim, *Electron. Mater. Lett.* **11**, 481 (2015).
6. D. H. Kim and S. Y. Lee, *Thin Solid Films* **536**, 327 (2013).
7. S. Q. Hussain, S. Kim, S. Ahn, H. Park, A. H. T. Le, S. Lee, Y. Lee, J. H. Lee and J. Yi, *Met. Mater. Int.* **20**, 565 (2014).
8. K. Kim, S. Lee and W. Cho, *Mater. Sci. Eng. B* **178**, 811 (2013).
9. D. Kim, *Ceram. Int.* **40**, 1457 (2014).
10. H. M. Lee, Y. J. Lee, I. S. Kim, M. S. Kang, S. B. Heo, Y. S. Kim and D. Kim, *Vacuum* **86**, 1494 (2012).
11. J. C. Kim, C. H. Shin, C. W. Jeong, Y. J. Kwon, J. H. Park and D. Kim, *Nucl. Instrum. Meth. B* **268**, 131 (2010).